Journal of Mathematical Chemistry 13(1993)33–43

Ten microseconds in the life of a superhelix

Giuseppe Chirico[a], Ulrike Kapp[b], Konstanin Klenin[c], Werner Kremer[b] and Jörg Langowski[b,1]

[a]*Dipartimento di Fisica, Sez. Struttura della Materia, Università di Milano, Via Celoria 16, I-20133 Milano, Italy*

[b]*EMBL, Grenoble Outstation, c/o ILL, 156X, F-38042 Grenoble Cedex, France*

[c]*Troitsk Institute of Innovational and Thermonuclear Research, Troitsk, Moscow Region 142092, Russia*

Dynamic light scattering measurement data of DNA topoisomers are compared with two different computer models: a Monte Carlo model and a Brownian dynamics model. First results on the kinetics of formation of a superhelix and on the influence of curved sequences on the dynamics of superhelical DNA are reported.

1. Introduction

DNA supercoiling is important for the structural organization of DNA in the cell. Many biological processes require an interaction of DNA sequences which are several hundreds of base pairs apart. Winding the double helix into a higher-order "superhelix" can bring such sequences close enough together so that they can interact through space, a protein molecule being the mediator (e.g. the binding of two *lac* operator sequences by the same repressor molecule [1]). DNA does not have to be circular to form a superhelix; it is sufficient that the two ends of a piece of DNA cannot twist with respect to each other, e.g. if they are bound to structural proteins in the cell.

The conformation of a superhelix is determined by its linking number difference ΔLk, which is connected to the deviation of the total twist from equilibrium ΔTw and the writhe of Wr of the helix axis through the relationship [2]

$$\Delta\mathrm{Lk} = \mathrm{Wr} + \Delta\mathrm{Tw}. \tag{1}$$

The superhelical density σ, used later in the text, is the linking number difference per double-helical turn at equilibrium, or for a DNA of N_b base pairs (bp) and a helix repeat of 10.5 bp/turn

$$\sigma = \Delta\mathrm{Lk} \times 10.5/N_b. \tag{2}$$

Typically, $\sigma = -0.05$ to -0.07 for native superhelical DNA.

[1]To whom correspondence should be addressed.

The repartition of the elastic energy into twist and writhe depends on mechanical properties of the DNA filament, such as its bending and twisting rigidity, its diameter, and the local equilibrium of the DNA helix axis, which may be straight or curved. For a consistent picture of the function of superhelical DNA in the cell, it is important to know how the fundamental physical properties of DNA determine its structure and dynamics and therefore the thermodynamics and kinetics of intramolecular interactions in DNA.

Data on the solution structure and dynamics of DNA have been collected with a variety of techniques such as fluorescence depolarization anisotropy decay, electric dichroism and birefringence, dynamic light scattering, and others (for a review, see ref. [3]). Our own work has concentrated on studies of the structure and dynamics of superhelical DNA using dynamic light scattering (DLS) [4–7]. Presently, the only way to connect DLS and many other dynamical measurements on DNA to fundamental physical parameters of the molecule, including its sequence-specific properties, is through numerical simulations.

Physical studies of superhelical DNA require sufficient quantities of samples of defined superhelicity. Up to now, only rather broad distributions of topoisomers could be produced by selective relaxation with topoisomerase in the presence of intercalators, a serious experimental drawback which we tried to overcome by developing a method for the separation of DNA topoisomers on reversed phase chromatography [8,9]. Using this technique, we can produce topoisomer distributions that contain only two to three major components.

DLS measurements on these topoisomers yield the translational diffusion coefficient D_t of the DNA and information on its internal motions [4]. We compare our data with predictions made by two different computer models: a Monte Carlo model developed by Vologodskii, Klein and co-workers [10,11] for predicting the average solution *structure* of the molecule, and a Brownian dynamics model developed in our group for predicting the *dynamics* of the DNA. Both models are based only on physical parameters of the DNA known previously from other techniques (bending and torsional rigidity, hydrodynamic diameter, excluded volume diameter). We report here first results on the kinetics of formation of a superhelix, and on the influence of curved sequences on the dynamics of superhelical DNA.

2. Methods

2.1. PREPARATION OF TOPOISOMERS

For physical studies on superhelical DNA, one needs sufficient material of well-defined superhelical density. In most previous studies, superhelical DNA was relaxed with topoisomerase I in the presence of intercalators, resulting in a population of topoisomers with defined negative superhelical density [27]. We have recently developed a procedure for separating further such topoisomer distributions on HPLC [8,9]. With this method, we obtain very narrow topoisomer distributions from pUC18 plasmid DNA (2687 base pairs) with only two to three components.

2.2. DLS MEASUREMENTS

For determining hydrodynamic properties of DNA as a function of superhelix density, we used dynamic light scattering (DLS). DLS measures the Brownian motion of molecules in solution by analyzing the fluctuations of scattered laser light via the autocorrelation function (ACF) of the scattered light intensity [12]. We have shown in previous work that the ACF of the scattered light from solutions of superhelical and linear plasmid DNAs can be decomposed into two principal components: a slow decay corresponding to the translational diffusion of the center of mass of the molecule, and a fast one corresponding to the internal diffusion of subsegments of the DNA with respect to each other [4].

The translational diffusion coeficient D_t of a molecule can be interpreted in a very straightforward way as a hydrodynamic radius R_h

$$R_h = k_B T / D_t.$$

Several models exist for computing the diffusion coefficients of models composed of spherical beads [13]. In the following, we shall discuss the dependence of D_t on superhelical density σ and compare the experimental values with those obtained from a Monte Carlo model.

2.3. MONTE CARLO SIMULATIONS

The Monte Carlo model used in the calculation was that described by Vologodskii et al. [11], modified to accomodate sequence-depending bending (Klenin and Langowski, in preparation).

pUC18 has a total length of 2687 base pairs, or a contour length of $2687 \times 0.34 = 914$ nm. The chain actually modelled consisted of 96 segments of 9.54 nm each, each segment being further subdivided into three spherical beads of 3.184 nm diameter. This choice of bead diameter has been shown to reproduce the hydrodynamic properties of DNA [14]. The slight deviation of the total chain contour length (2694 instead of 2687 base pairs, or 0.26%) is due to the discrete nature of the model and considered to be negligible. The Kuhn length of DNA is known to be 100 nm for ionic strengths >0.01 M and was set to this value; the torsional rigidity α was assumed to be either 4×10^{-12} dyn cm, which is a value typically measured for linear DNA in fluorescence polarization decay (FPA) experiments [15], or $\alpha = 8.8 \times 10^{-12}$ dyn cm, which was obtained from cyclization data of small DNA fragments by Horowitz and Wang [16]. The "effective helix diameter", taking into account excluded volume, was set to 0.02 Kuhn lengths, or 2 nm. The diffusion coefficients of the chain configurations were computed using the algorithm described by de Haën et al. [13], which we found to predict very accurately the diffusion coefficient of DNA bead-chain models [14].

All programs were written in FORTRAN 77, and the simulations were run on the EMBL Outstation's Stardent 3000 with two P3 processors, using the compiler's vectorization option.

2.4. BROWNIAN DYNAMICS SIMULATIONS

Some applications of Brownian dynamics (BD) to studies of DNA internal motions have already been described, notably through the work of Allison and co-workers [17–20]. Those simulations have been confined to linear DNA chains. Inclusion of the torsional constraints and simulations of superhelical DNAs was possible with the algorithm described there, but very expensive in CPU time. Thus, we recently developed a Brownian dynamics model based on a second-order algorithm described by Iniesta and Garcia de la Torre [21]. This method speeds-up the computation by a factor of three to five on linear DNAs.

We have now included the torsional constraints and torsional-bending coupling into the model. The full theory will be described in a forthcoming paper; here, we outline only the most important points.

A covalently closed DNA molecule is modelled as a string of N beads of diameter $d = 2\sigma_b$ and spaced by l_s. N is chosen such that the DNA contour length $L_c = Nl_s$. In our preceding work [14], the beads formed a contiguous chain with $l_s = 2\sigma_b = 3.184$ nm, or 9.3 base pairs. This value was proposed by Hagerman and Zimm [22] to reproduce the hydrodynamic diameter of a B-DNA double helix. In the work described here, we also use a non-contiguous model for the simulation of longer chains.

Each bead, representing a subcomponent of the chain, has a body-fixed coordinate (bfc) system associated with it. We define $\Phi_{j,j+1} = (\alpha_{j,j+1}, \beta_{j,j+1}, \gamma_{j,j+1})$ as the Eulerian angle that orients the $j+1$ subcomponent in the bfc system of the j subcomponent. The center of bead $j+1$ is always placed on the z-axis of the bfc system of bead j. Since the molecule is a closed circle, there exists no preference for choosing the first and last Nth bead, thus the index $j+N$ will be equal to the index j throughout the following calculations; e.g. $\Phi_{N,N+1} = \Phi_{N,1}$.

The potential energy of the molecule is composed of four contributions:

$$U^{tot} = U^b + U^s + U^t + U^{ex}. \tag{3}$$

U^b, U^s, U^t and U^{ex} denote the bending, stretching, torsional and excluded volume potentials:

$$U^b = \frac{k_B T}{2\zeta^2} \sum_{j=1}^{N} \beta_j^2, \tag{4a}$$

$$U^s = \frac{k_B T}{2\delta^2} \sum_{j=1}^{N} (|\boldsymbol{b}_j| - l_s)^2, \tag{4b}$$

$$U^{t} = \frac{k_B T}{2\xi^2} \sum_{j=1}^{N} (\alpha_j + \gamma_j)^2, \tag{4c}$$

$$U^{ex} = 4k_B T\, \varepsilon \sum_{i<j}^{N} \left[\left(\frac{\sigma}{b_{i,j}} \right)^{12} - \left(\frac{\sigma}{b_{i,j}} \right)^{6} \right] \Phi\left(\frac{\sigma}{b_{i,j}} \right) \quad \Phi(x) = \begin{cases} 1, & x \geq 1, \\ 0, & x < 1, \end{cases} \tag{4d}$$

where $k_B T/\zeta^2$, $k_B T/\delta^2$ and $k_B T/\xi^2$ are the bending, stretching and torsional force constants, $\boldsymbol{b}_j = \boldsymbol{r}_{j+1} - \boldsymbol{r}_j$, and $b_{i,j} = |\boldsymbol{r}_i - \boldsymbol{r}_j|$. The values of ζ and δ are chosen as in ref. [14], ξ corresponds to a torsional rigidity $\alpha = 8 \times 10^{-12}$ dyn cm, and $\varepsilon = 10^{-6}$. σ in eq. (4d) is an excluded volume parameter; for $\sigma/b_{i,j} = 3$, $U_{ex} = k_B T$.

The Langevin equations for the translational and rotational Brownian motion of a molecule composed of N beads of equal mass m in an incompressible continuum solvent can be expressed in convenient form for numerical integration through the second-order approximation discussed by Iniesta and Garcia de la Torre [21]. In this formalism, the position of the ith bead after a simulation time step δt is computed as follows:

$$\boldsymbol{r}_i(t + \delta t) = \boldsymbol{r}_i(t) + \frac{1}{2k_B T} \sum_{j=1}^{N} \left[\mathbf{D}_{ij}(t + \delta t)\mathbf{F}_j(t + \delta t) + \mathbf{D}_{ij}(t)\mathbf{F}_j(t) \right] \delta t + \boldsymbol{R}_i(t) \tag{5}$$

$$i = 1, \ldots, N,$$

where $\mathbf{D}_{ij}(t)$ is the Rotne–Prager diffusion tensor [23] describing the hydrodynamic interaction between beads i and j. The viscosity of the medium was assumed to be that of water. $\mathbf{F}_j(t)$ is the force acting on bead j, and the random displacements $\boldsymbol{R}_i(t)$ obey the relation

$$\langle \boldsymbol{R}_i(t) : \boldsymbol{R}_j(t) \rangle = [\mathbf{D}_{ij}(t + \delta t) + \mathbf{D}_{ij}(t)]\, \delta t; \qquad \langle \boldsymbol{R}_i(t) \rangle = 0 \tag{6}$$

$$i, j = 1, \ldots, N.$$

The torsional displacement of the ith bead after a time step δt is

$$\Phi_i(t + \delta t) = \Phi_i(t) + \frac{1}{2k_B T} D^R [T_i(t + \delta t) + T_i(t)]\, \delta t + S_i(t), \tag{7}$$

where $T_i(t)$ is the torque acting on the ith bfc system, D^R the rotational diffusion coefficient of the ith subcomponent, and the random rotation S_i has the following statistical properties:

$$S_i(t) = \chi(2D^R\, \delta t)^{0.5}; \quad \langle \chi \rangle = 0.0; \quad \langle \chi^2 \rangle = 1.0. \tag{8}$$

In the simulations, we used $D^R = 7.03 \times 10^7\ s^{-1}$, which is the value for a cylinder of 2.4 nm diameter and 3.184 nm length at 293 K in water.

The forces $\boldsymbol{F}_i$ and the torques T_i are computed from the derivatives of the respective potentials,

$$\begin{aligned} \boldsymbol{F}_i &= -\frac{\partial}{\partial \boldsymbol{r}_i} U^{\mathrm{tot}} = \boldsymbol{F}_i^{\mathrm{b}} + \boldsymbol{F}_i^{\mathrm{s}} + \boldsymbol{F}_i^{\mathrm{t}} + \boldsymbol{F}_i^{\mathrm{ex}}, \\ T_i &= -\frac{\partial}{\partial \Phi_i} U^{\mathrm{t}}. \end{aligned} \tag{9}$$

More details about the calculations will be published in a forthcoming paper [26]. For the moment, we stress that for a correct treatment of the topological constraints of a closed circular DNA, it is necessary to include the bending–torsional coupling force $\boldsymbol{F}_i^{\mathrm{t}} = -\partial U^{\mathrm{t}}/\partial \boldsymbol{r}_i$ in the simulations.

The linking number difference ΔLk is included in the simulation by taking as a starting point a planar circular molecule with each set of Eulerian angles Φ_j defined by the relations

$$\begin{aligned} \alpha_j &= -2\pi(j-1)\Delta\mathrm{Lk}/N, \\ \beta_j &= 2\pi j/N, \\ \gamma_j &= 2\pi j \Delta\mathrm{Lk}/N. \end{aligned} \tag{10}$$

In this configuration, all the initial torsional stress is contained in twisting and none in writhing. The torsion angle between beads N and 1 is automatically taken mod 2π by confining all Eulerian angles to the interval $[-\pi, \pi]$ at each simulation step. For the ΔLk values used in our computations, all α_j and γ_j are always small enough so that this procedure does not lead to artifacts. In order to check the consistency of the simulation, we verified that the relationship (1) was always fulfilled by the total twist and writhe of the chain. Small deviations from (1) – not exceeding 1% on the average – were probably due to the fact that (4c) holds strictly only in the limit of zero bending angle, and to the approximation of a smoothly bent chain by a finite number of segments.

3. Results

3.1. DLS MEASUREMENTS AND MONTE CARLO SIMULATIONS

The translational diffusion coefficient D_{t} increases with ΔLk, reflecting the compaction of the DNA molecule as its configuration changes from relaxed circle to superhelix (fig. 1). D_{t} approaches a plateau value of $5.0 \times 10^{-12}\,\mathrm{m^2\,s^{-1}}$ for $\Delta\mathrm{Lk} \leq -10$ ($\sigma < -0.04$). Co-plotted in fig. 1 are some data from earlier measurements on pUC8 (2717 bp), which has almost the same size as pUC18 and shows very similar behavior.

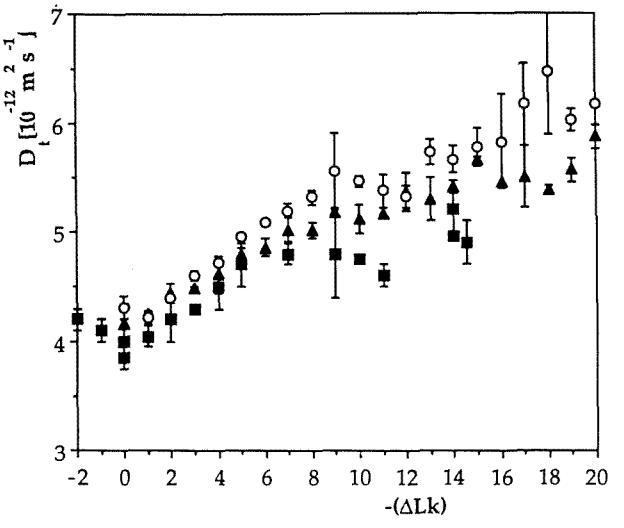

Fig. 1. Translational diffusion coefficient of topoisomers of pUC8 (2686 bp) as a function of the number of negative superhelical turns (ΔLk). (■) experimental data; (▲) Monte Carlo simulation with a torsional constant $\alpha = 4 \times 10^{-12}$ dyn cm; (○) with $\alpha = 8.8 \times 10^{-12}$ dyn cm.

The agreement between the experimental data and the Monte Carlo simulations is very good. Two choices exist for the torsional rigidity: $\alpha = 4 \times 10^{-12}$ dyn cm, which is a value typically measured for linear DNA in fluorescence polarization decay (FPA) experiments [15], and $\alpha = 8.8 \times 10^{-12}$ dyn cm, which is obtained from cyclization data of small DNA fragments by Horowitz and Wang [16]. The agreement is slightly better for the low value of α.

3.2. MONTE CARLO SIMULATIONS OF THE INFLUENCE OF LOCAL CURVATURE ON SUPERHELICAL STRUCTURE

There is evidence that curved DNA sequences localize in the end loops of superhelical DNA [24]. To understand the consequences of this phenomenon, we have calculated the effect of permanent bends with the Monte Carlo model. The DNA chain modelled was the same as in the previous calculations, with a permanent 120° bend approximated by two 60° bends between segments 47, 48 and 49.

Figure 2 shows the formation probability of a segment being at the apex of an end loop as a function of chain position. The control with no bends shows no preferential loop formation, as expected. For the model chain with a bend, we find a maximum of the loop formation probability exactly at the position of the permanent bend. Furthermore, the loop formation probability over a range of approximately 400 base pairs to both sides of the permanent bend is significantly reduced with respect to the control. At a distance of approximately 800 bp from the bend, a

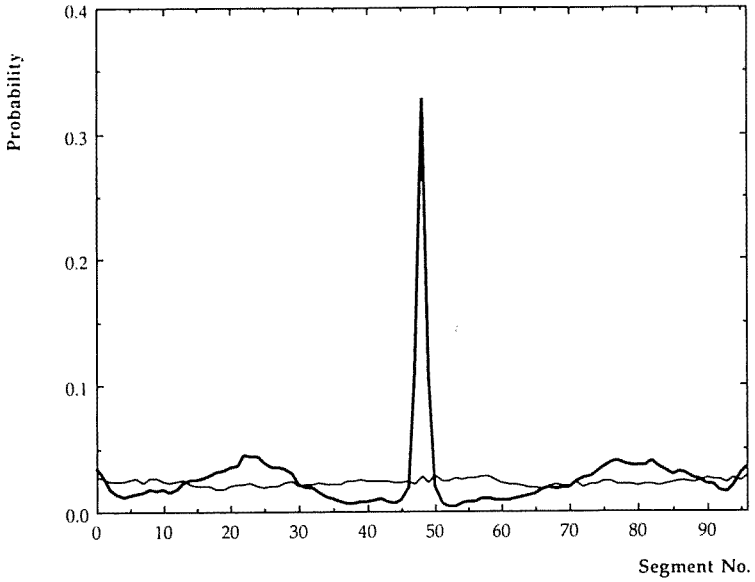

Fig. 2. End loop formation probability versus chain position for a 96-segment model of pUC18 with and without permanent bends. (−) 60° bends between segments 47, 48 and 49; (—) no bends.

secondary maximum of the loop formation appears, which may be due to an increase in the number of branched structures; this hypothesis is presently being tested.

The consequence of this finding is that a permanent bend arranges the DNA sequences to both sides of it in a fixed fashion, thus defining possible DNA−DNA interactions. We have some preliminary experimental evidence that DNAs with permanent bends have a lower degree of internal motion than those without bends [25].

3.3. BROWNIAN DYNAMICS SIMULATIONS

The DNA molecule is modelled as a contiguous chain of 30 beads of diameter $d = 3.184$ nm, as explained in section 2. The total length of the chain thus corresponded to 281 base pairs. The motions of circular chains of linking number difference $\Delta Lk = -2$ and -5, corresponding to superhelical densities of $\sigma = -0.07$ and $\sigma = -0.19$ were simulated for approximately 10 μs, starting from a flat circular configuration.

Figure 3 shows some typical configurations of the two DNA chains during the course of the simulation. Since the bending tension in these small circles is much higher than in typical superhelical plasmid DNAs of several thousand bp length, we had to employ much higher superhelix densities than the $\sigma = -0.05$ to -0.07 found in natural DNAs in order to form superhelical turns. The circle with $\Delta Lk = -2$ starts to form a single superhelical turn only at the very end of the simulation, while for $\Delta Lk = -5$ the formation of the first turn takes about 1 μs. After two superhelical turns have formed, the amplitude of the shape fluctuations

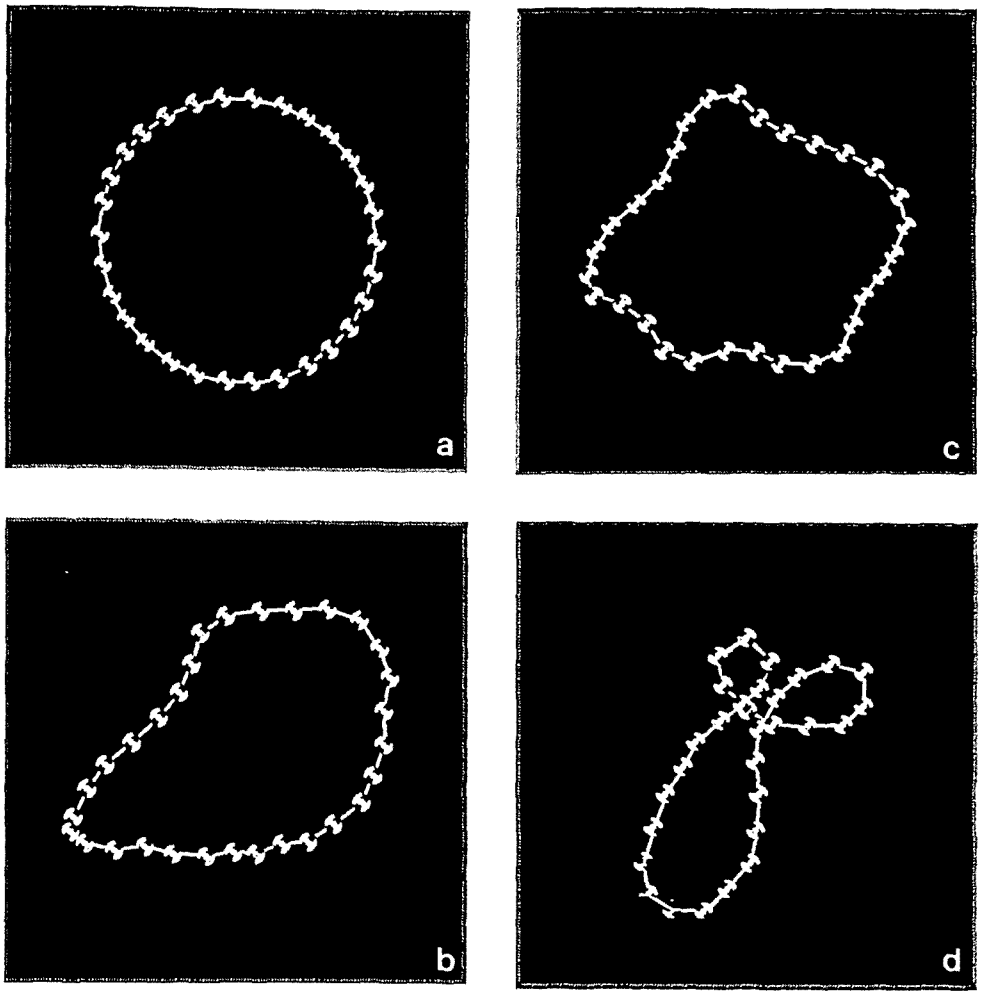

Fig. 3. Brownian dynamics calculation of a 281 bp DNA circle simulated by 30 spherical beads. (a) Starting configuration, (b) $\Delta Lk = -2$ after 10 μs, (c) $\Delta Lk = -5$ after 0.1 μs, (d) $\Delta Lk = -5$ after 10 μs. ΔLk = linking number difference (number of superhelical turns).

of the $\Delta Lk = -5$ circle decreases visibly; this is in agreement with our experimental finding that the internal motion amplitude of superhelical DNA is much smaller than that of linear DNA [5].

We note that the formation of the interwound superhelix of the $\Delta Lk = -5$ circle proceeds through a transient toroidal state which is formed after approximately 0.1 μs (fig. 3c). A similar mechanism has now been observed in simulations of longer plasmid DNAs (data not shown).

4. Conclusion

On extremely purified samples of DNA topoisomers, we could measure the translational diffusion coefficient of superhelical DNA as a function of its linking number and compare the experimental data with predicted values from Monte Carlo simulations. The good agreement between theory and experiment confirms the validity of the Monte Carlo model by Vologodskii et al. [11] for structural predictions.

The Monte Carlo model furthermore predicts that permanently curved DNA sequences localize with preference in the end loops of interwound superhelices, a fact which is also seen experimentally [24]. The consequence of this localization is that the mobility of DNA segments in the neighborhood of the permanent bend is severely restricted; over a distance of approximately 400 base pairs to both sides of the permanent bend, the loop formation probability is strongly reduced. This means that the relative orientation of DNA segments to both sides of the permanent bend should be non-random; sequences placed symmetrically with respect to the bend will have a higher probability of interaction than other sequences. First experimental evidence for this prediction comes from DLS measurements, which show a reduced overall internal mobility of superhelical DNA when a permanent bend is present in the molecule.

Brownian dynamics (BD) simulations can be used to compute the kinetics of superhelix formation and interactions in superhelical DNA. With a new BD model based on a second-order algorithm [14,19], and with the inclusion of torsional potentials and torsional–bending coupling, we were ablé for the first time to simulate the dynamics of a 281 base pair DNA circle for a total time of 10 μs. The results reported here will be extended to predict the dynamics for longer supercoils, which are also accessible experimentally, and to study the effect of permanent bends on the dynamics. First data on 1100 base pair circles are now available [26].

Note added in proof

After submission of this paper, another group has presented a model of the dynamics of DNA supercoiling that is based on a B-Spline representation of the space curve of the DNA double helix [28,29]. Their model predicts the main structural features of the final equilibrium state, and gives qualitative information about the kinetics of supercoiling; however, since no viscous damping or hydrodynamic interaction have been included in that work, the kinetics cannot be calculated on an absolute time scale and slow periodic oscillations around the equilibrium are seen in the simulations which could be overdamped in a viscous medium like water. These issues are addressed in a forthcoming paper [26], which also contains more detailed information about the algorithms used here.

Acknowledgement

This work was supported by DFG Grant La 500/3-3 and NATO Grant CRG 910239 to JL.

References

[1] M. Ptashne, Nature 322(1986)697.
[2] J.H. White, Am. J. Math. 91(1969)693.
[3] P.J. Hagerman, Annu. Rev. Biophys. Biophys. Chem. 17(1988)265.
[4] J. Langowski, U. Giesen and C. Lehmann, Biophys. Chem. 25(1986)191.
[5] J. Langowski, Biophys. Chem. 27(1987)263.
[6] J. Langowski and U. Giesen, Biophys. Chem. 34(1989)9.
[7] J. Langowski and R. Bryan, in: *Neutron, X-ray and Light Scattering*, ed. P. Lindner and Th. Zemb (Elsevier, Amsterdam, 1991).
[8] U. Kapp and J. Langowski, Anal. Biochem. 206(1992)293.
[9] J. Langowski, W. Kremer and U. Kapp, in: *DNA Structure*, Vol. 211, Meth. Enzymology, ed. D. Lilley and J. Dahlberg, in press.
[10] A.V. Vologodskii, V.V. Anshelevich, A.V. Lukashin and M.D. Frank-Kamenetskii, Nature 280(1979)294.
[11] K.V. Klein, A.V. Vologodskii, V.V. Anshelevich, A.M. Dykhne and M.D. Frank-Kamenetskii, J. Mol. Biol. 217(1991)413.
[12] B.J. Berne and R. Pecora, *Dynamic Light Scattering* (Wiley, New York, 1976).
[13] C. de Haën, R.A. Easterly and D. Teller, Biopolymers 22(1983)1133.
[14] G. Chirico and J. Langowski, Macromolecules 25(1992)769.
[15] J.C. Thomas, S.A. Allison, C.J. Appellof and J.M. Schurr, Biophys. Chem. 12(1980)177.
[16] D.S. Horowitz and J.C. Wang, J. Mol. Biol. 173(1984)75.
[17] S.A. Allison and J.A. McCammon, Biopolymers 23(1984)363.
[18] S.A. Allison, Macromolecules 19(1986)118.
[19] S.A. Allison, S.S. Sorlie and R. Pecora, Macromolecules 23(1990)1110.
[20] R.G. Lewis, S.A. Allison, D. Eden and R. Pecora, J. Chem. Phys. 89(1988)2490.
[21] A. Iniesta and J. Garcia de la Torre, J. Chem. Phys. 92(1990)2015.
[22] P.J. Hagerman and B.H. Zimm, Biopolymers 20(1981)1481.
[23] J. Rotne and S. Prager, J. Chem. Phys. 50(1969)4831.
[24] C.H. Laundon and J.D. Griffith, Cell 52(1988)545.
[25] W. Kremer, U. Kapp and J. Langowski, in preparation.
[26] G. Chirico and J. Langowski, J. Mol. Biol., submitted.
[27] C.K. Singleton and R.D. Wells, Anal. Biochem. 122(1982)253.
[28] T. Schlick and W.K. Olson, J. Mol. Biol. 223(1992)1089.
[29] T. Schlick and W.K. Olson, Science 257(1992)1110.